Cardiology in the Young

cambridge.org/cty

Original Article

***Jing Wang, Rui-Qi Guo, and Jian-Ying Guo contributed equally to this work.**

Cite this article: Wang J, Guo R-Q, Guo J-Y, Zuo L, Lei C-H, Shao H, Wang L-F, Zhang Y-M, Liu L-W. (2018). Investigation of myocardial dysfunction using three-dimensional speckle tracking echocardiography in a genetic positive hypertrophic cardiomyopathy Chinese family. *Cardiology in the Young* **28**: 1106–1114. doi: 10.1017/S1047951118000860

Received: 3 September 2017
Revised: 1 April 2018
Accepted: 2 May 2018

Key words:
Hypertrophic cardiomyopathy; myocardial dysfunction; three-dimensional speckle tracking echocardiography; multiple mutations

Author for correspondence:
Prof. L.-W. Liu, Department of Ultrasound, Xijing Hospital, Fourth Military Medical University, Xi'an, Shaanxi 710032, China.
Tel: +86 29 8477 5443; Fax: +86 29 8324 4121;
E-mail: liuliwen@fmmu.edu.cn

CAMBRIDGE UNIVERSITY PRESS

Investigation of myocardial dysfunction using three-dimensional speckle tracking echocardiography in a genetic positive hypertrophic cardiomyopathy Chinese family

Jing Wang[1,*], Rui-Qi Guo[1,*], Jian-Ying Guo[2,*], Lei Zuo[1], Chang-Hui Lei[1], Hong Shao[1,3], Li-Feng Wang[4], Yan-Min Zhang[5] and Li-Wen Liu[1]

[1]Department of Ultrasound, Xijing Hospital, Fourth Military Medical University, Xi'an, Shaanxi, China, [2]Military Patients Reception Center, Xijing Hospital, Fourth Military Medical University, Xi'an, Shaanxi, China, [3]Department of Cardiology, Xijing Hospital, Fourth Military Medical University, Xi'an, Shaanxi, China, [4]Department of Biochemistry and Molecular Biology, Fourth Military Medical University, Xi'an, Shaanxi, China and [5]Xi'an Children's Hospital of Xi'an Jiaotong University, Children's Research Institute of Shaanxi Province, Xi'an, Shaanxi, China

Abstract

Background: We previously reported four heterozygous missense mutations of *MYH7*, *KCNQ1*, *MYLK2*, and *TMEM70* in a single three-generation Chinese family with dual Long QT and hypertrophic cardiomyopathy phenotypes for the first time. However, the clinical course among the family members was various, and the potential myocardial dysfunction has not been investigated. *Objectives:* The objective of this study was to investigate the echocardiographic and electrocardiographic characteristics in a genetic positive Chinese family with hypertrophic cardiomyopathy and further to explore the association between myocardial dysfunction and electric activity, and the identified mutations. *Methods:* A comprehensive echocardiogram – standard two-dimensional Doppler echocardiography and three-dimensional speckle tracking echocardiography – and electrocardiogram were obtained for members in this family. *Results:* As previously reported, four missense mutations – *MYH7*-H1717Q, *KCNQ1*-R190W, *MYLK2*-K324E, and *TMEM70*-I147T – were identified in this family. The *MYH7*-H1717Q mutation carriers had significantly increased left ventricular mass indices, elevated E/e' ratio, deteriorated global longitudinal stain, but enhanced global circumferential and radial strain compared with those in non-mutation patients (all $p < 0.05$). The *KCNQ1*-R190W carriers showed significantly prolonged QTc intervals, and the *MYLK2*-K324E mutation carriers showed inverted T-waves (both $p < 0.05$). However, the *TMEM70*-I147T mutation carriers had similar echocardiography and electrocardiographic data as non-mutation patients. *Conclusions:* Three of the identified four mutations had potential pathogenic effects in this family: *MYH7*-H1717Q was associated with increased left ventricular thickness, elevated left ventricular filling pressure, and altered myocardial deformation; *KCNQ1*-R190W and *MYLK2*-K324E mutations were correlated with electrocardiographic abnormalities reflected in long QT phenotype and inverted T-waves, respectively.

Hypertrophic cardiomyopathy is the most common inheritable myocardial disorder with an estimated prevalence of 1:500 in the general population.[1] It is inherited as an autosomal dominant trait in 50–60% of cases, with over 1400 mutations identified in a range of cardiac sarcomere genes.[2,3] These mutations cause an increase in myocyte stress, eventually leading to myocyte hypertrophy, fibre disarray, and interstitial fibrosis. It has been proposed that contractile force of individual cardiac myocyte is impaired because of these microscopic abnormalities, resulting in intrinsic functional abnormalities, despite apparently normal systolic function by conventional measurements.[4,5] The advent of three-dimensional speckle tracking echocardiography enables a more accurate assessment of left ventricular myocardial shortenings in all three spatial dimensions, which potentially provides better mechanistic insight into underlying myocardial dysfunction in patients with hypertrophic cardiomyopathy.

At present, clinical genetic testing in patients with hypertrophic cardiomyopathy can provide valuable information on diagnosis and early identification of individuals at risk, especially among family members.[6,7] Our group had also reported four heterozygous missense mutations, *MYH7*-H1717Q, *KCNQ1*-R190W, *MYLK2*-K324E, and *TMEM70*-I147T, in a single three-generation Chinese family with overlapping Long QT and hypertrophic cardiomyopathy phenotypes.[8] However, the disease expression among the family members was markedly different, and the potential myocardial dysfunction has not been investigated in our

previous study. Therefore, we conducted this study to further evaluate the myocardial deformation using three-dimensional speckle tracking echocardiography, as well as electrocardiographic features in the family members, and to explore the association between myocardial dysfunction and electric activity, and the identified mutations.

Materials and methods

Study population

This study was conducted at a tertiary-care medical centre, in which patients were referred for extensive assessment on hypertrophic cardiomyopathy. The study protocol was approved by the institution's research ethical committees. As previously described, eight members of the three-generation Chinese family with hypertrophic cardiomyopathy were enrolled and written informed consent was obtained from all patients. For the children <16 years old, written informed consents were obtained from their parents.

According to the European Society of Cardiology guideline,[7] the clinical diagnosis of hypertrophic cardiomyopathy is established on a maximal left ventricular wall thickness ⩾ 15 mm. In case of children <18 years old, the diagnosis of hypertrophic cardiomyopathy requires a wall thickness ⩾ 2 SD above the predicted mean (z-score ⩾ 2) for age, gender, or body size. The clinical diagnosis of hypertrophic cardiomyopathy in first-degree relatives of patients with unequivocal disease is based on the presence of otherwise unexplained increased left ventricular wall thickness ⩾ 13 mm.

Transthrocic echocardiography

Transthoracic echocardiography (iE33; Philips Medical System, Bothell, Washington, United States of America) was performed using a multi-frequency matrix probe with patients in the left lateral decubitus position.

Standard echocardiography

Standard two-dimensional and Doppler images were acquired in accordance with guidelines of the American Society of Echocardiography.[9] The uniformity of left ventricular wall thickness was visually assessed in all left ventricular segments by examining the parasternal short-axis levels and the apical views to identify regions with disproportionately increased thickness. If a relatively thickened segment was identified, the location was noted and maximal left ventricular wall thickness was measured. Left ventricular end-diastolic diameter was measured and left ventricular mass was estimated and divided by the body surface area to derive left ventricular mass index. The left ventricular ejection fraction was calculated using biplane Simpson's method. The left ventricular outflow tract pressure gradient was measured with continuous-wave Doppler in the apical five-chamber view both at rest and during a Valsalva manoeuver. Left atrial transverse diameter was measured in the apical four-chamber view as the distance from the midpoint of the interatrial septum to the lateral left atrial wall. Left atrial volume was assessed by area-length method and indexed to body surface area to derive left atrial volume index. The early (E), late (A) diastolic peak velocities of mitral inflow and the systolic (s'), early (e') diastolic peak velocities of mitral annulus were measured by pulsed-wave Doppler and tissue Doppler imaging. Subsequently, E/A ratio and E/e' ratio were calculated to evaluate the left ventricular diastolic function.[10]

Three-dimensional speckle tracking echocardiography

The three-dimensional echocardiographic imaging was acquired from the apical position. The full-volume acquisition, in which four adjacent wedge-shaped subvolumes were captured with four consecutive cardiac cycles, was performed during a single breath-hold to minimise the artefact between the subvolumes. Moreover, the temporal and spatial resolutions of the images were optimised by decreasing the depth and adjusting the sector width to ensure that the entire left ventricle was included within the pyramidal scan volume. The offline analysis of the resultant three-dimensional speckle tracking echocardiography data sets was performed using Tom-Tec 4.0 analysis software (Tom-Tec Imaging Systems Gmbh, Unterschleissheim, Bayern, Germany). After setting two reference points at the base of the left ventricle at the mitral valve level and one at the apex on two orthogonal apical views at the end-diastolic frame, the software automatically tracked the endocardial and epicardial contours on subsequent frames through the entire cardiac cycle in three different vectors simultaneously. The endocardial contour and myocardial thickness were manually adjusted when necessary to optimise boundary position and tracking. Thus, using the standard 16-segmental model, time curves of global and segmental strain, including its four principal components (circumferential, radial, longitudinal, and three-dimensional strains), were obtained.

Statistical analysis

Statistical analysis was performed with SPSS version 19.0 (SPSS Inc, Chicago, Illinois, United States of America). Continuous variables were expressed as mean ± standard deviation and categorical variables as percentages. Comparisons of continuous variables between mutation carriers and non-mutation carriers were performed using Student's t-test or Mann–Whitney U test as appropriate and χ^2 test for categorical variables.

Intra-observer and inter-observer variabilities of three-dimensional data were evaluated in all family members involved by two independent investigators. Both observers were blinded to the previous measurements. Intra-observer and inter-observer variabilities were evaluated by means of intra-class correlation coefficients (ICC). A value of $p < 0.05$ was considered significant.

Results

Clinical characteristics and genotypes of the family pedigree

As previously described, eight patients in this family aged from 7 to 79 years (4 male and 4 female) were examined. Figure 1 shows the pedigree structure, and their clinical characteristics are summarised in Table 1. Briefly, the proband (II-9) was a 38-year-old man with two transient and self-terminating episodes of syncope. Electrocardiographic recordings showed a late-onset inverted T-wave pattern, ST depression, and prolonged QTc interval (469 ms). Asymmetric left ventricular hypertrophy – predominant involvement of the interventricular septum – was evident in echocardiography, with a left ventricular mass index of 109.55 g/m^2, maximal left ventricular wall thickness of 24 mm, and left ventricular ejection fraction of 70%. The proband's father (I-1) and mother (I-2) all experienced the episodes of vertigo.

https://doi.org/10.1017/S1047951118000860 Published online by Cambridge University Press

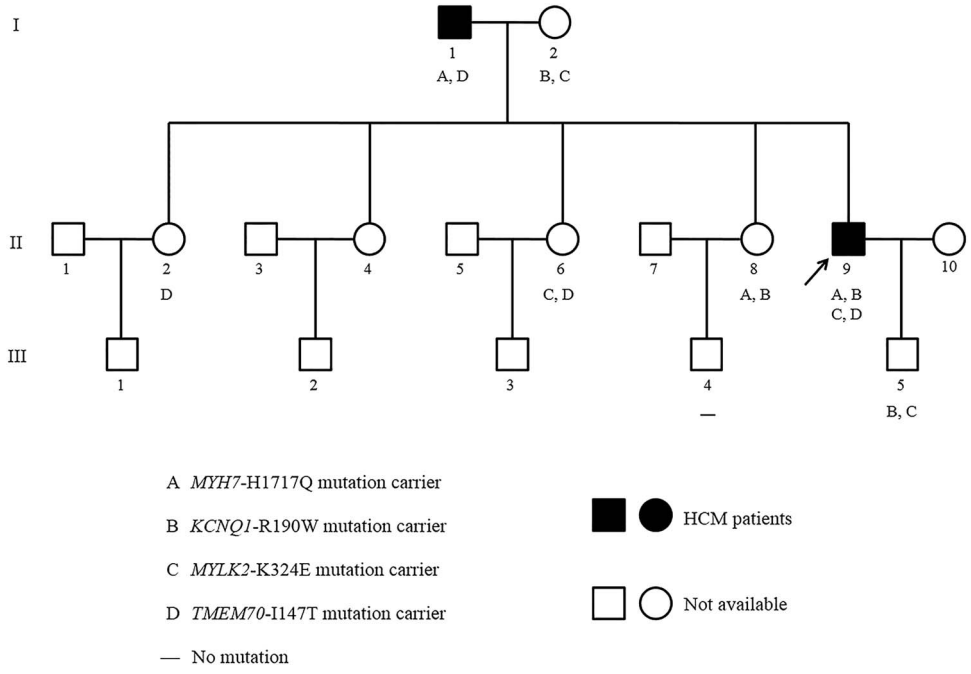

Figure 1. Pedigree of the family with phenotypic and genotypic information. Male family members are indicated by squares; female family members are indicated by circles; the solid symbols represent the individuals diagnosed with hypertrophic cardiomyopathy (HCM); and the unavailable individuals are represented by open symbols. In addition, the proband is marked with a black arrow. The genotype for each individual is noted below the symbol, where available. The absence of mutations is indicated by a "–" sign. A: *MYH7*-H1717Q; B: *KCNQ1*-R190W; C: *MYLK2*-K324E; D: *TMEM70*-I147T.

There were no clinical symptoms, syncope, or sudden cardiac death in the remaining family members.

Four heterozygous missense mutations were detected in this family, as previously reported, including the following: A, *MYH7*-H1717Q – c.5151T > A within exon 35 of *MYH7* resulting in a histidine to glutamine substitution p.H1717Q in the myosin heavy-chain β isoform; B, *KCNQ1*-R190W – c.568C > T within exon 3 of *KCNQ1* resulting in an arginine to tryptophan substitution p.R190W in the Kv7.1, voltage-gated potassium channel; C, *MYLK2*-K324E – c.970A > G within exon 6 of *MYLK2* resulting in a lysine to glutamic acid substitution p.K324E in myosin light-chain kinase 2; and D, *TMEM70*-I147T – c.440T > C within exon 3 of *TMEM70* resulting in an isoleucine to threonine substitution p.I147T in transmembrane protein 70. The proband (II-9) carried all four mutations. Patients I-1, I-2, II-6, II-8, and III-5 carried two mutations in the form of A-D, B-C, C-D, A-B, and B-C, respectively. Patient II-2 carried mutation D only, whereas patient III-4 did not carry any of the above-detected mutations (Table 1). Subsequently, they were divided into two subgroups: subgroup of mutation carriers and subgroup of non-mutation patients.

Comparisons of echocardiographic and electrocardiographic data between the subgroups

Among the eight screened patients, the proband's mother (I-2) was shown to have unexplained heart failure, and echocardiography showed nearly normal wall thickness with a maximal left ventricular wall thickness of 12 mm and left ventricular global hypokinesia with left ventricular ejection fraction of 46% (Table 1). Thus, it is unknown whether there was impaired systolic function that may be associated with hypertrophic cardiomyopathy-related genes or such abnormal myocardial contractility was owing to other causes such as coronary artery disease. Therefore, she was excluded and the remaining seven patients were retained for subsequent analysis.

MYH7-H1717Q mutation carriers versus non-mutation patients

In all, three patients (I-1, II-8, and II-9) carried the *MYH7*-H1717Q mutation, which is the most common pathogenic gene of hypertrophic cardiomyopathy. The left ventricular mass index, e', and E/e' ratio showed a clear trend to higher values in the *MYH7*-H1717Q mutation carriers than non-mutation patients ($p < 0.05$, Table 2) as expected, whereas both subgroups had comparable left ventricular end-diastolic diameter, left ventricular ejection fraction, left ventricular outflow tract pressure gradient, left atrial dimension, left atrial volume index, s', and E/A ratio.

Among the global myocardial mechanics parameters measured by three-dimensional speckle tracking echocardiography, there was a trend towards increased global circumferential and radial strain in the *MYH7*-H1717Q mutation carriers, whereas the global longitudinal strain in the mutation carriers was significantly lower, as compared with the non-mutation patients (all $p < 0.05$, Table 2, Figs 2a and 3). Other parameters including three-dimensional stain, twist, and torsion showed no significant differences in the two subgroups. On the regional myocardial mechanics aspect, the circumferential strain at the mid segment of the anterior wall, the radial strain at the basal segments of the posteroseptal inferior walls, and apical segments of lateral anterior walls were significantly increased in the *MYH7*-H1717Q mutation carriers. In contrast, the longitudinal strain of almost basal segments, mid segments of the anteroseptal anterior walls, and apical segment of the septal wall were all decreased in the mutation carriers (all $p < 0.05$, Table 3). Moreover, three-dimensional strain values of all 16 segments were comparable between the two subgroups.

https://doi.org/10.1017/S1047951118000860 Published online by Cambridge University Press

Table 1. Clinical, genetic, electrocardiographic, and echocardiographic characteristics of the family pedigree.

Patient ID	Gender/age (years)	BSA (m^2)	Symptoms	Genotype	Electrocardiography						Echocardiography			
					Heart rhythm	HR (bpm)	QTc (ms)	Inverted T-wave	ST depression	Q-wave*	Q-wave**	LVEF (%)	LVMI (g/m^2)	MLWT (mm)	Number of thickened segments
I-1	M/76	1.57	Vertigo	A, D	SR	57	423	–	–	Yes	–	62	94.27	14	2
I-2	F/79	1.66	Vertigo	B, C	SR	85	519	Yes	Yes	–	Yes	46	78.31	12	–
II-2	F/56	1.54	–	D	SR	66	420	–	–	–	–	54	60.39	9	–
II-6	F/48	1.47	–	C, D	SR	64	399	Yes	–	–	–	57	66.67	8	–
II-8	F/45	1.66	–	A, B	SR	72	451	–	–	–	Yes	59	84.34	11	–
II-9	M/38	1.78	Syncope	A, B, C, D	SR	62	469	Yes	Yes	–	Yes	70	109.55	24	3
III-4	M/21	1.81	–	No mutation	SR	68	392	–	–	Yes	–	62	59.67	9	–
III-5	M/7	1.02	–	B, C	SR	90	450	Yes	–	–	Yes	65	50.98	6	–

A = *MYH7*-H1717Q; B = *KCNQ1*-R190W; C = *MYLK2*-K324E; D = *TMEM70*-I147T; BSA = body surface area; HR = heart rate; LVEF = left ventricular ejection fraction; LVMI = left ventricular mass index; MLVWT = maximal left ventricular wall thickness; SR = sinus rhythm

*Q-wave <30 ms in duration and ⩾ 1 mm in depth in II, III, and aVF leads

**Q-wave <30 ms in duration and ⩾ 1 mm in depth in V4-V5 leads

In addition, there were no significant differences in electrocardiographic parameters between *MYH7*-H1717Q mutation carriers and non-mutation patients (Table 2).

The results suggested that *MYH7*-H1717Q mutation correlated with the increased left ventricular thickness, elevated left ventricular filling pressure, and abnormal myocardial mechanics in this family.

KCNQ1-R190W mutation carriers versus non-mutation patients

Of the seven family members, three patients (II-8, II-9, and III-5) carried *KCNQ1*-R190W. The *KCNQ1*-R190W mutation carriers and non-mutation patients had comparable standard two-dimensional Doppler echocardiographic parameters and global and regional myocardial shortening measured with three-dimensional speckle tracking echocardiography (Table 2, Fig 2b, and Supplemental Table 1).

With respect to the electrocardiographic parameters, we have previously reported that the QTc intervals of the *KCNQ1*-R190W mutation carriers were significantly prolonged as compared with the non-mutation carriers ($p < 0.05$, Table 2), and patients II-9 and III-5 showed clinical long QT syndrome. It suggested that *KCNQ1*-R190W mutation was probably involved in a long QT phenotype in this family. In addition, there were no significant differences in other electrocardiographic parameters.

MYLK2-K324E mutation carriers versus non-mutation patients

Three patients (II-6, II-9, and III-5) in the involved seven family members carried the *MYLK2*-K324E mutation. Similar to our findings in subgroups of the *KCNQ1*-R190W mutation, standard two-dimensional Doppler echocardiographic parameters, as well as global and regional myocardial deformation derived from three-dimensional speckle tracking echocardiography analysis, were all indistinguishable between the *MYLK2*-K324E mutation carriers and non-mutation patients (Table 2, Fig 2c, and Supplemental Table 2).

As previously reported, the *MYLK2*-K324E mutation carriers showed inverted T-waves in multiple precordial leads, whereas T-waves were upright in the non-mutation patients ($p < 0.05$, Table 2). It suggested that *MYLK2*-K324E mutation might be responsible for abnormal repolarisation in this family.

TMEM70-I147T mutation carriers versus non-mutation patients

In this family, four patients (I-1, II-2, II-6, and II-9) carried the *TMEM70*-I147T mutation encoding transmembrane protein 70, which was linked to isolated adenosine triphosphate synthase deficiency and neonatal mitochondrial encephalocardiomyopathy.[11,12] Both echocardiographic parameters and electrocardiographic data showed no significant differences between the *TMEM70*-I147T mutation carriers and non-mutation patients (Table 2, Fig 2d, and Supplemental Table 3), which indicated that *TMEM70*-I147T may be less pathogenic in this family.

Reproducibility of three-dimensional speckle tracking echocardiography measurements

Intra-observer agreement for three-dimensional speckle tracking echocardiography parameters was fairly good: global circumferential strain (ICC = 0.91), global longitudinal strain (ICC = 0.94), global radial strain (ICC = 0.93), three-dimensional strain (ICC = 0.91), twist (ICC = 0.89), and torsion (ICC = 0.85) (all $p < 0.01$). Similar results were noted for inter-observer agreement: global circumferential strain (ICC = 0.83), global longitudinal

https://doi.org/10.1017/S1047951118000860 Published online by Cambridge University Press

Table 2. Comparisons of electrocardiographic and echocardiographic parameters between mutation carriers and non-mutation patients.

	A (*MYH7*-H1717Q)			B (*KCNQ1*-R190W)			C (*MYLK2*-K324E)			D (*TMEM70*-I147T)		
	Mutation	Non-mutation	p Value	Mutation	Non-mutation	p Value	Mutation	Non-mutation	p Value	Mutation	Non-mutation	p Value
Standard echocardiography												
LVEDD (mm)	42 ± 3	42 ± 4	NS	41 ± 4	43 ± 3	NS	41 ± 3	44 ± 3	NS	42 ± 1	43 ± 5	NS
LVEF (%)	64 ± 6	60 ± 5	NS	65 ± 6	59 ± 4	NS	64 ± 7	59 ± 4	NS	61 ± 7	62 ± 3	NS
LVMI (g/m^2)	96.05 ± 12.70	59.43 ± 6.45	0.004	81.62 ± 29.38	70.25 ± 16.32	NS	75.73 ± 30.32	74.67 ± 17.38	NS	82.72 ± 23.16	65.00 ± 17.31	NS
LVOT-PG (mmHg)	5 ± 2	4 ± 2	NS	5 ± 2	4 ± 2	NS	4 ± 3	4 ± 2	NS	5 ± 2	3 ± 1	NS
LA dimension (mm)	37 ± 4	30 ± 5	NS	34 ± 8	33 ± 2	NS	33 ± 11	34 ± 3	NS	35 ± 5	32 ± 6	NS
LAVI (ml/g^2)	28.43 ± 6.03	19.22 ± 5.19	NS	25.25 ± 11.19	21.60 ± 2.92	NS	21.96 ± 8.25	24.07 ± 7.19	NS	23.24 ± 4.63	23.06 ± 10.83	NS
e' (cm/s)	7.1 ± 1.1	12.1 ± 3.2	0.044	10.2 ± 4.2	9.8 ± 3.6	NS	10.5 ± 4.0	9.6 ± 3.7	NS	8.2 ± 1.9	12.4 ± 4.1	NS
s' (cm/s)	7.4 ± 1.0	7.5 ± 0.9	NS	7.6 ± 1.0	7.4 ± 0.9	NS	7.5 ± 1.2	7.4 ± 0.7	NS	7.4 ± 1.0	7.5 ± 0.9	NS
E/A ratio	1.23 ± 0.55	1.43 ± 0.52	NS	1.65 ± 0.30	1.11 ± 0.52	NS	1.58 ± 0.41	1.16 ± 0.53	NS	1.09 ± 0.47	1.68 ± 0.32	NS
E/e' ratio	11.4 ± 1.4	7.0 ± 0.6	0.002	10.5 ± 2.8	7.7 ± 1.7	NS	8.8 ± 2.3	9.0 ± 3.0	NS	9.0 ± 2.0	8.8 ± 3.5	NS
3D speckle tracking echocardiography												
GCS (%)	− 35.14 ± 2.99	− 28.54 ± 1.12	0.009	− 33.87 ± 4.35	− 29.49 ± 2.92	NS	− 31.95 ± 5.88	− 30.93 ± 2.91	NS	− 32.09 ± 5.14	− 30.41 ± 2.47	NS
GRS (%)	46.37 ± 1.69	40.44 ± 3.30	0.038	45.96 ± 2.39	40.75 ± 3.68	NS	42.11 ± 5.67	43.63 ± 3.17	NS	41.88 ± 4.93	44.45 ± 2.67	NS
GLS (%)	− 16.64 ± 0.89	− 22.02 ± 2.39	0.015	− 19.20 ± 3.74	− 20.10 ± 3.60	NS	− 19.49 ± 3.58	− 19.89 ± 3.76	NS	− 18.48 ± 3.28	− 21.37 ± 3.28	NS
3D Strain (%)	− 37.15 ± 2.18	− 35.46 ± 2.63	NS	− 36.19 ± 2.30	− 36.18 ± 2.86	NS	− 35.49 ± 3.15	− 36.71 ± 2.07	NS	− 37.08 ± 3.03	− 35.00 ± 0.29	NS
Twist (°)	14.04 ± 4.35	12.61 ± 3.15	NS	13.03 ± 4.83	13.37 ± 2.84	NS	12.87 ± 4.96	13.48 ± 2.63	NS	14.49 ± 3.91	11.53 ± 2.26	NS
Torsion (°/cm)	1.97 ± 0.53	1.83 ± 0.46	NS	1.87 ± 0.54	1.90 ± 0.46	NS	1.83 ± 0.60	1.93 ± 0.40	NS	2.04 ± 0.54	1.68 ± 0.24	NS
Electrocardiography												
QTc (ms)	448 ± 23	415 ± 26	NS	457 ± 11	409 ± 15	0.006	439 ± 36	422 ± 24	NS	428 ± 30	431 ± 34	NS
Inverted T-wave (%)	67	50	NS	67	25	NS	100	0	0.029	50	33	NS
ST depression (%)	33	0	NS	33	0	NS	33	0	NS	25	0	NS

3D = three-dimensional; e' = early diastolic mitral annular velocity; E/A ratio = ratio of early to late mitral inflow velocity; E/e' ratio = ratio of early diastolic mitral inflow velocity to early diastolic mitral annular velocity; GCS = global circumferential strain; GLS = global longitudinal strain; GRS = global radial strain; LA = left atrial; LAVI = left atrial volume index; LVEDD = left ventricular end-diastolic diameter; LVEF = left ventricular ejection fraction; LVMI = left ventricular mass index; LVOT-PG = left ventricular outflow tract pressure gradient; NS = no significant difference; s' = systolic mitral annular velocity

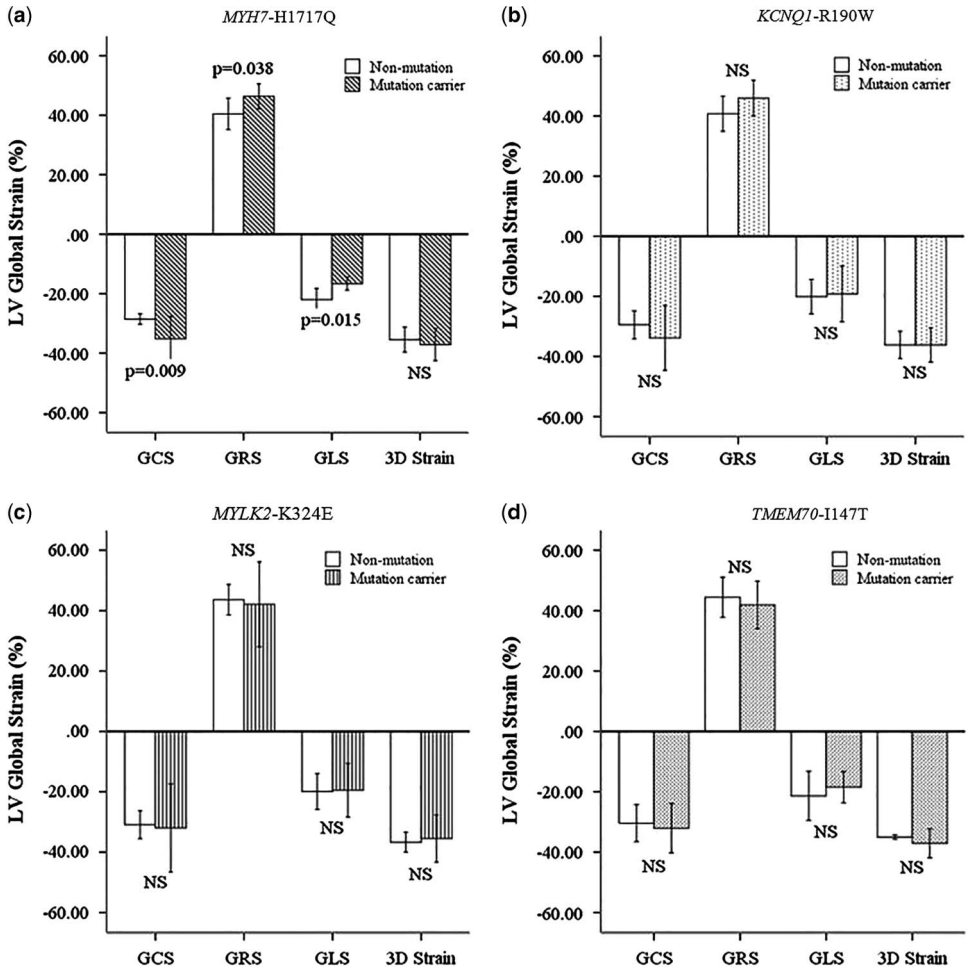

Figure 2. Left ventricular myocardial strain derived from three-dimensional (3D) speckle tracking analysis in mutation carriers versus non-mutation patients. (*a*) The comparisons of left ventricular global strain between the *MYH7*-H1717Q mutation carriers and non-mutation patients; (*b*) the comparisons of left ventricular global strain between the *KCNQ1*-R190W mutation carriers and non-mutation patients; (*c*) the comparisons of left ventricular global strain between the *MYLK2*-K324E mutation carriers and non-mutation patients; and (*d*) the comparisons of left ventricular global strain between the *TMEM70*-I147T mutation carriers and non-mutation patients. GCS = global circumferential strain; GLS = global longitudinal strain; GRS = global radial strain; LV = left ventricular; NS = no significant difference.

strain (ICC = 0.91), global radial strain (ICC = 0.86), three-dimensional strain (ICC = 0.84), twist (ICC = 0.80), and torsion (ICC = 0.78), respectively (all $p < 0.01$).

Discussion

This study was designed to investigate the echocardiographic – standard two-dimensional Doppler echocardiography and three-dimensional speckle tracking echocardiography – and electrocardiographic characteristics in a three-generation Chinese family with hypertrophic cardiomyopathy, and to explore the potential association between myocardial dysfunction, electrical activity, and the identified mutations. We found that the *MYH7*-H1717Q mutation was associated with increased left ventricular thickness, elevated left ventricular filling pressure, and altered myocardial deformation. More specifically, in the *MYH7*-H1717Q mutation carriers, global myocardial deformation is attenuated in the longitudinal direction and enhanced in the circumferential and radial directions. We also found that the *KCNQ1*-R190W and *MYLK2*-K324E mutations were correlated with electrocardiographic abnormalities reflected in long QT phenotype and inverted T-waves.

The potential effects of mutations on echocardiography and electrocardiography in this family

We have previously reported four missense mutations detected in this family. *MYH7* is the most common pathogenic gene of hypertrophic cardiomyopathy, encoding beta-cardiac myosin heavy chain (MHC-β) expressed primarily in the heart.[13] In this family, the increased left ventricular mass index, elevated E/e' ratio, and altered myocardial shortenings were detected in the *MYH7*-H1717Q mutation carriers. Thus, we speculated that *MYH7*-H1717Q had pathogenic effects in left ventricular hypertrophy, diastolic dysfunction, and myocardial mechanics; it is potential to be a disease-causing mutation in this family.

KCNQ1 and *MYLK2* were two other identified mutations. *KCNQ1* encodes a voltage-gated potassium channel (Kv7.1) required for the repolarisation phase of the cardiac action potential,[14] and *MYLK2* encodes myosin light-chain kinase 2, a calcium-independent enzyme, mainly expressed in skeletal muscle.[15] As previously reported, the family members with *KCNQ1*-R190W mutation showed prolonged QTc compared with non-mutation patients, which confirmed the investigation that loss-of-function *KCNQ1* mutations are associated with long QT phenotype. Moreover, those with the *MYLK2*-K342E mutations

https://doi.org/10.1017/S1047951118000860 Published online by Cambridge University Press

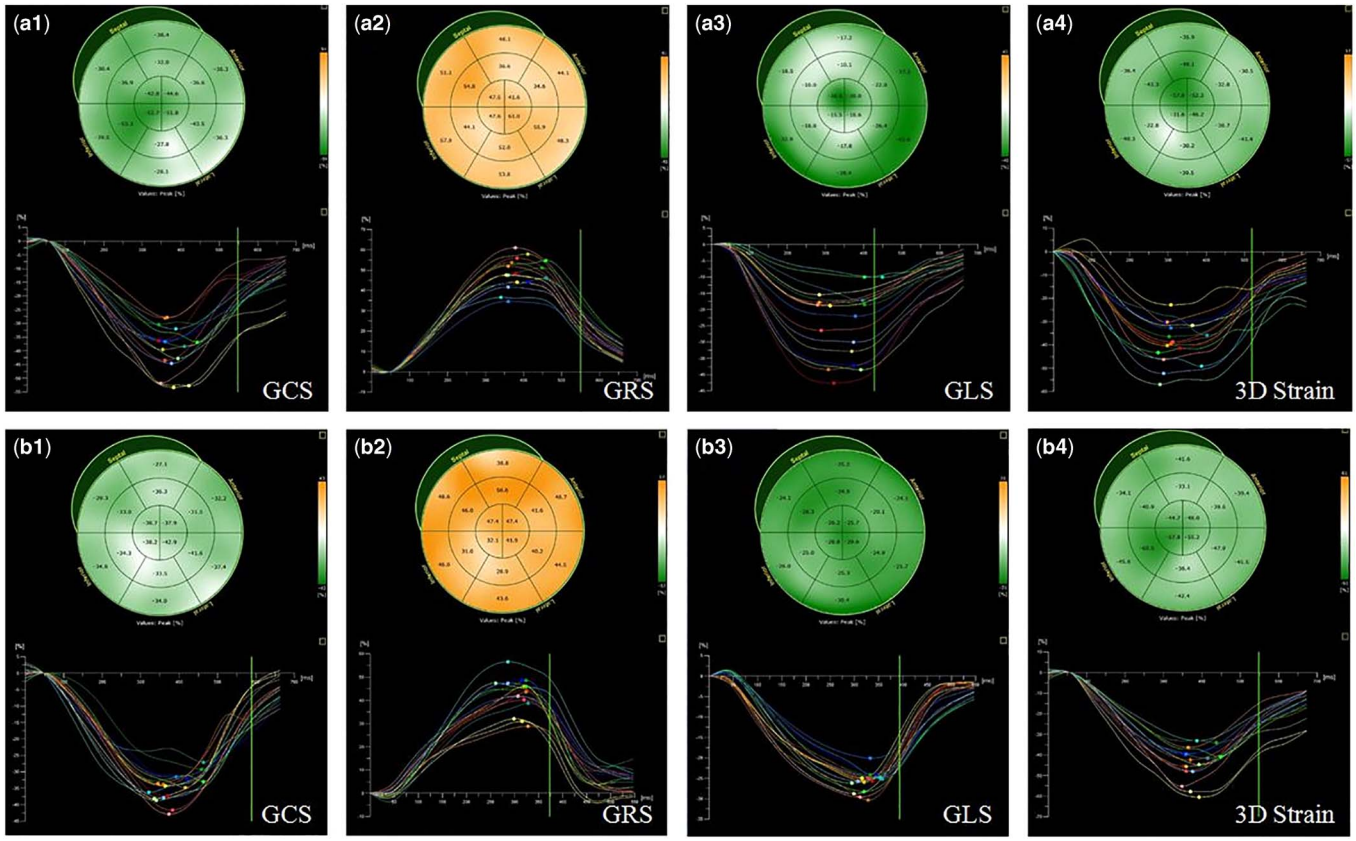

Figure 3. Representative three-dimensional (3D) strain curves of the 16 segments of left ventricle in (*a*) the *MYH7*-H1717Q mutation carrier (patient II-9) and (*b*) non-mutation patient (patient III-4). GCS = global circumferential strain; GLS = global longitudinal strain; GRS = global radial strain.

showed inverted electrocardiographic T-waves, indicating the potential role of *MYLK2*-K324E mutation in cardiac repolarisation abnormalities.

Three-dimensional speckle tracking analysis of left ventricular myocardial mechanics in hypertrophic cardiomyopathy

In hypertrophic cardiomyopathy, malfunctioning sarcomeric protein, myocyte hypertrophy, fibre disarray, increased loose interstitial, and replacement fibrosis are all thought to interfere with myocardial force generation, relaxation, and reduced energy use.[1,2,5] Although in most patients left ventricular systolic function is hyperdynamic with a high ejection fraction, hypertrophic cardiomyopathy causes non-uniformities in myofibre shortening and alters the pattern of myocardial deformation. In other words, hypertrophic cardiomyopathy is a paradoxical disorder of apparent increased contractility but reduced myocardial power at the molecular level.[16]

Three-dimensional speckle tracking echocardiography is a newly developed technique to evaluate the myocardial deformation, which relies on three-dimensional data sets and tracks the motion of speckles within a scanned volume, irrespective of direction. Validation studies[17,18] have confirmed its accuracy for the quantitative assessment of myocardial mechanics by using cardiac magnetic resonance as a reference method, suggesting that three-dimensional speckle tracking echocardiography has the potential to detect the subtle impairment of myocardial function.

In the present study, a notable attenuation of global longitudinal strain, measured by three-dimensional speckle tracking echocardiography, was observed in hypertrophic cardiomyopathy patients with *MYH7*-H1717Q mutation despite preserved ejection fraction, which was consistent with previous investigations.[19,20] We also found that myocardial deformation in the circumferential and radial directions were increased. These can be explained by the unique distribution of myocytes in disarray in patients with hypertrophic cardiomyopathy. It is noteworthy that myocytes in the subendocardium are responsible for most of the longitudinal deformation, whereas those in the subepicardium account for circumferential deformation. In hypertrophic cardiomyopathy, maximal myofibre disarray occurs in the inner region of the myocardium, and therefore myofibres in the subendocardium are likely to be the most impaired leading to decreased longitudinal deformation. However, myofibres in the subepicardium are the least affected by disarray,[21,22] which may compensate for the myocardial dysfunction from subendocardial region resulting in increased circumferential and radial deformation, as well as preservation in three-dimensional stain; that is, myocardial deformation in the circumferential and radial directions seems to be directly involved in the maintenance of left ventricular systolic performance in hypertrophic cardiomyopathy. Furthermore, this combination of opposite changes in the perpendicular components of strain was also seen in some of the hypertrophic segments in hypertrophic cardiomyopathy patients with *MYH7*-H1717Q mutation, which suggested that hypertrophic cardiomyopathy is a global myocardial disorder with more pronounced alternations in segments with a higher disease burden.

Although most patients may show preserved or even increased left ventricular contraction by conventional measurements, this

https://doi.org/10.1017/S1047951118000860 Published online by Cambridge University Press

Table 3. Comparisons of left ventricular regional strain derived between *MYH7*-H1717Q mutation carriers and non-mutation patients.

	CS (%)			RS (%)			LS (%)			3D strain (%)		
	Mutation	Non-mutation	p Value	Mutation	Non-mutation	p Value	Mutation	Non-mutation	p Value	Mutation	Non-mutation	p Value
Basal segments												
Posteroseptal	−28.84 ± 6.15	−20.74 ± 4.38	NS	39.30 ± 2.85	29.87 ± 7.25	0.034	−12.31 ± 4.11	−20.81 ± 3.06	0.025	−34.39 ± 1.71	−30.54 ± 5.78	NS
Lateral	−30.13 ± 1.95	−24.60 ± 6.14	NS	45.90 ± 1.71	40.87 ± 9.15	NS	−21.23 ± 3.48	−27.52 ± 5.88	NS	−35.27 ± 1.71	−32.43 ± 5.40	NS
Anterior	−33.66 ± 0.20	−29.96 ± 3.21	NS	44.73 ± 1.49	43.52 ± 4.37	NS	−17.12 ± 4.94	−25.20 ± 2.99	0.042	−29.76 ± 2.13	−33.76 ± 3.79	NS
Inferior	−35.22 ± 2.70	−26.86 ± 5.34	NS	48.72 ± 5.51	38.07 ± 3.37	0.024	−17.50 ± 4.14	−25.73 ± 2.39	0.020	−37.54 ± 2.50	−34.31 ± 2.69	NS
Anteroseptal	−25.64 ± 3.34	−22.42 ± 4.41	NS	34.11 ± 5.53	34.92 ± 3.38	NS	−9.69 ± 3.98	−23.72 ± 2.82	0.003	−29.31 ± 3.70	−31.43 ± 2.93	NS
Posterior	−27.55 ± 3.31	−21.52 ± 4.78	NS	43.98 ± 6.36	36.68 ± 7.17	NS	−20.99 ± 3.04	−29.37 ± 2.40	0.009	−33.58 ± 2.75	−31.68 ± 3.93	NS
Mid segments												
Posteroseptal	−45.16 ± 12.64	−38.06 ± 8.57	NS	52.54 ± 9.75	44.02 ± 9.68	NS	−16.37 ± 4.55	−17.55 ± 5.36	NS	−51.21 ± 9.15	−45.65 ± 5.16	NS
Lateral	−36.56 ± 2.82	−31.76 ± 4.60	NS	48.09 ± 5.17	44.45 ± 5.21	NS	−17.70 ± 7.56	−20.63 ± 5.62	NS	−39.29 ± 1.53	−35.48 ± 5.61	NS
Anterior	−34.02 ± 2.94	−28.99 ± 4.37	0.034	44.07 ± 2.25	41.71 ± 6.34	NS	−17.27 ± 0.33	−22.02 ± 3.60	0.034	−30.38 ± 0.68	−32.60 ± 4.30	NS
Inferior	−42.17 ± 4.63	−34.22 ± 4.22	NS	53.43 ± 3.11	44.84 ± 6.17	NS	−20.23 ± 1.56	−20.64 ± 5.08	NS	−44.53 ± 8.86	−43.44 ± 6.67	NS
Anteroseptal	−40.24 ± 4.43	−32.52 ± 5.28	NS	46.81 ± 2.73	41.33 ± 5.18	NS	−13.63 ± 1.62	−18.68 ± 2.58	0.032	−44.31 ± 8.79	−37.18 ± 5.14	NS
Posterior	−34.83 ± 2.69	−28.00 ± 3.84	NS	47.34 ± 4.36	40.30 ± 7.38	NS	−18.38 ± 4.41	−19.86 ± 6.09	NS	−34.82 ± 1.65	−35.34 ± 3.69	NS
Apical segments												
Septal	−43.53 ± 13.21	−36.75 ± 4.82	NS	49.36 ± 9.58	45.53 ± 5.54	NS	−13.55 ± 1.34	−21.83 ± 7.53	0.034	−44.03 ± 10.01	−41.31 ± 4.50	NS
Lateral	−39.13 ± 6.22	−32.14 ± 2.74	NS	53.61 ± 6.05	44.07 ± 3.51	0.045	−19.31 ± 1.78	−19.52 ± 4.96	NS	−37.44 ± 6.91	−39.89 ± 8.97	NS
Anterior	−40.97 ± 7.81	−32.90 ± 3.87	NS	51.73 ± 3.80	42.73 ± 3.67	0.034	−16.05 ± 2.47	−18.64 ± 2.32	NS	−40.42 ± 7.22	−36.31 ± 5.73	NS
Inferior	−42.30 ± 5.30	−35.84 ± 4.67	NS	52.37 ± 2.85	48.30 ± 7.35	NS	−17.16 ± 2.02	−22.50 ± 5.68	NS	−40.47 ± 3.34	−43.73 ± 9.90	NS

CS = circumferential strain; LS = longitudinal strain; NS = no significant difference; RS = radial strain.

macroscopic compensation may eventually fail with the progress of reduced power at the microscopic units in hypertrophic cardiomyopathy.[16,23] At present, the relationship between the pathological types, severity, and myocardial deformation derived from three-dimensional speckle tracking echocardiography in patients with hypertrophic cardiomyopathy has not been established. Regardless, the decline in longitudinal strain may herald transition into the "burnt-out" phase of hypertrophic cardiomyopathy and may be of great value in monitoring patients.

Limitations

Some limitations should be underlined in the current study. The main limitation was inherent to the small number of patients, and the presented results originated just from a Chinese pedigree. As the pathogenic mechanisms of the identified mutations remained speculative, a larger-scale study with more patients in multiple pedigrees is required to confirm the results. Moreover, our study still lacked a "gold standard" such as cardiac magnetic resonance to validate the three-dimensional speckle tracking echocardiography technique, which would be added in the future studies.

Conclusions

In the present study, we sought to investigate the echocardiographic and electrocardiographic characteristics in a three-generation Chinese family with hypertrophic cardiomyopathy and four identified mutations. We found that three of them had potential pathogenic effects in this family: *MYH7*-H1717Q mutation was associated with increased left ventricular thickness, elevated left ventricular filling pressure, and altered myocardial deformation; *KCNQ1*-R190W and *MYLK2*-K324E mutations were correlated with long QT phenotype and inverted T-waves, respectively. In addition, the finding that global myocardial deformation is attenuated in the longitudinal direction and enhanced in the circumferential and radial directions in *MYH7*-H1717Q mutation carriers warrants further clinical studies.

Supplementary materials. To view supplementary material for this article, please visit https://doi.org/10.1017/S1047951118000860

Acknowledgements. The authors extend their heartfelt thanks to Prof. Yu-Xin Fan in US Baylor College of Medicine and Dr Bo Wang in the Department of Ultrasound of Xijing Hospital for their support to this study.

Financial Support. This work was supported by International S &T Cooperation Program of China (2014DFA31980) and National Natural Science Foundation of China (81671693 to L Liu, 81601498 to J Wang).

Conflicts of Interest. None.

References

1. Maron BJ. Hypertrophic cardiomyopathy: a systematic review. JAMA 2002; 287: 1308–1320.
2. Bos JM, Towbin JA, Ackerman MJ. Diagnostic, prognostic, and therapeutic implications of genetic testing for hypertrophic cardiomyopathy. J Am Coll Cardiol 2009; 54: 201–211.
3. Ho CY. Genetics and clinical destiny: improving care in hypertrophic cardiomyopathy. Circulation 2010; 122: 2430–2440.
4. McLeod CJ, Bos JM, Theis JL, et al. Histologic characterization of hypertrophic cardiomyopathy with and without myofilament mutations. Am Heart J 2009; 158: 799–805.
5. Marian AJ. Pathogenesis of diverse clinical and pathological phenotypes in hypertrophic cardiomyopathy. Lancet 2000; 355: 58–60.
6. Ackerman MJ, Priori SG, Willems S, et al. HRS/EHRA expert consensus statement on the state of genetic testing for the channelopathies and cardiomyopathies: this document was developed as a partnership between the Heart Rhythm Society (HRS) and the European Heart Rhythm Association (EHRA). Europace 2011; 13: 1077–1109.
7. Authors/Task Force members, Elliott PM, Anastasakis A, et al. 2014 ESC Guidelines on diagnosis and management of hypertrophic cardiomyopathy: the Task Force for the Diagnosis and Management of Hypertrophic Cardiomyopathy of the European Society of Cardiology (ESC). Eur Heart J, 2014; 35: 2733-2779.
8. Wang L, Zuo L, Hu J, et al. Dual LQT1 and HCM phenotypes associated with tetrad heterozygous mutations in KCNQ1, MYH7, MYLK2, and TMEM70 genes in a three-generation Chinese family. Europace 2016; 18: 602–609.
9. Lang RM, Badano LP, Mor-Avi V, et al. Recommendations for cardiac chamber quantification by echocardiography in adults: an update from the American Society of Echocardiography and the European Association of Cardiovascular Imaging. J Am Soc Echocardiogr 2015; 28: 1–39.e14.
10. Nagueh SF, Appleton CP, Gillebert TC, et al. Recommendations for the evaluation of left ventricular diastolic function by echocardiography. J Am Soc Echocardiogr 2009; 22: 107–133.
11. Diodato D, Invernizzi F, Lamantea E, et al. Common and novel TMEM70 mutations in a cohort of Italian patients with mitochondrial encephalocardiomyopathy. JIMD Rep 2015; 15: 71–78.
12. Atay Z, Bereket A, Turan S, et al. A novel homozygous TMEM70 mutation results in congenital cataract and neonatal mitochondrial encephalocardiomyopathy. Gene 2013; 515: 197–199.
13. Núñez L, Gimeno-Blanes JR, Rodríguez-García MI, et al. Somatic MYH7, MYBPC3, TPM1, TNNT2, and TNNI3 mutations in sporadic hypertrophic cardiomyopathy. Circ J 2013; 77: 2358–2365.
14. Barsheshet A, Goldenberg I, O-Uchi J, et al. Mutations in cytoplasmic loops of the KCNQ1 channel and the risk of life-threatening events: implications for mutation-specific response to β-blocker therapy in type 1 long-QT syndrome. Circulation 2012; 125: 1988–1996.
15. Davis JS, Hassanzadeh S, Winitsky S, et al. The overall pattern of cardiac contraction depends on a spatial gradient of myosin regulatory light chain phosphorylation. Cell 2001; 107: 631–641.
16. Carasso S, Yang H, Woo A, et al. Systolic myocardial mechanics in hypertrophic cardiomyopathy: novel concepts and implications for clinical status. J Am Soc Echocardiogr 2008; 21: 675–683.
17. Kleijn SA, Brouwer WP, Aly MF, et al. Comparison between three-dimensional speckle-tracking echocardiography and cardiac magnetic resonance imaging for quantification of left ventricular volumes and function. Eur Heart J Cardiovasc Imaging 2012; 13: 834–839.
18. Seo Y, Ishizu T, Enomoto Y, et al. Validation of 3-dimensional speckle tracking imaging to quantify regional myocardial deformation. Circ Cardiovasc Imaging 2009; 2: 451–459.
19. Kansal MM, Lester SJ, Surapaneni P, et al. Usefulness of two-dimensional and speckle tracking echocardiography in "Gray Zone" left ventricular hypertrophy to differentiate professional football player's heart from hypertrophic cardiomyopathy. Am J Cardiol 2011; 108: 1322–1326.
20. Baccouche H, Maunz M, Beck T, et al. Differentiating cardiac amyloidosis and hypertrophic cardiomyopathy by use of three-dimensional speckle tracking echocardiography. Echocardiography 2012; 29: 668–677.
21. Wang TT, Kwon HS, Dai G, et al. Resolving myoarchitectural disarray in the mouse ventricular wall with diffusion spectrum magnetic resonance imaging. Ann Biomed Eng 2010; 38: 2841–2850.
22. Urbano-Moral JA, Rowin EJ, Maron MS, et al. Investigation of global and regional myocardial mechanics with 3-dimensional speckle tracking echocardiography and relations to hypertrophy and fibrosis in hypertrophic cardiomyopathy. Circ Cardiovasc Imaging 2014; 7: 11–19.
23. Bing W, Knott A, Redwood C, et al. Effect of hypertrophic cardiomyopathy mutations in human cardiac muscle alpha-tropomyosin (Asp175Asn and Glu180Gly) on the regulatory properties of human cardiac troponin determined by in vitro motility assay. J Mol Cell Cardiol 2000; 32: 1489–1498.